Bioorganic & Medicinal Chemistry 19 (2011) 985–993

Contents lists available at ScienceDirect

Bioorganic & Medicinal Chemistry

journal homepage: www.elsevier.com/locate/bmc

Synthesis and characterization of 5-hydroxymethyl-5-methyl-pyrroline *N*-oxide and its derivatives

Klaus Stolze [a,*], Natascha Rohr-Udilova [b], Anjan Patel [c], Thomas Rosenau [c]

[a] *Molecular Pharmacology and Toxicology Unit, Department of Biomedical Sciences, University of Veterinary Medicine Vienna, Veterinärplatz 1, A-1210 Vienna, Austria*
[b] *Division of Gastroenterology and Hepatology, Department of Internal Medicine III, Medical University of Vienna, Währinger Gürtel 18-20, A-1090 Vienna, Austria*
[c] *Department of Chemistry, University of Natural Resources and Life Sciences (BOKU), Muthgasse 18, A-1190 Vienna, Austria*

ARTICLE INFO

Article history:
Received 6 June 2010
Revised 17 November 2010
Accepted 20 November 2010
Available online 26 November 2010

Keywords:
EPR
Spin trapping
DMPO derivatives
Cyclodextrin
Superoxide

ABSTRACT

Synthesis and spin trapping behavior of three novel DMPO derivatives, namely 5-hydroxymethyl-5-methyl-pyrroline *N*-oxide (HMMPO), 5-(2-furanyl)-oxymethyl-5-methyl-pyrroline *N*-oxide (FMMPO), and 5-(2-pyranyl)-oxymethyl-5-methyl-pyrroline *N*-oxide (PMMPO) towards different oxygen- and carbon-centered radicals are described. The stabilizing effect of a series of cyclodextrins on the superoxide adducts was tested.

1. Introduction

Previous studies about DEPMPO and EMPO derivatives[1–7] were focused on the stability of superoxide adducts as well as investigations of mitochondria targeted spin traps[8–10] bearing positively charged phosphonium groups. Based on these studies we were aiming at synthesizing EMPO derivatives with a function to which a mitochondria targeting group could be readily attached in a single step. Unfortunately, the synthesis of 5-ethoxycarbonyl-4-hydroxymethyl-5-methyl-pyrroline *N*-oxide (the analogue of the previously reported 5-diethoxyphosphoryl-4-hydroxymethyl-5-methyl-1-pyrroline *N*-oxide, 4-HMDEPMPO[8,9]) is not straightforward, and several attempts to synthesize this compound in pure form have failed in our hands.[11] We therefore decided to first develop strategies involving different protective groups for the hydroxyl groups starting from simple related model compounds. In this study we report the synthesis of 5-hydroxymethyl-5-methyl-pyrroline *N*-oxide (HMMPO), a DMPO derivative having an extra hydroxyl group as an anchor group where specific functionalities can be attached thereby imposing a site-specific reactivity of the trap. We decided to investigate the effects of tetrahydrofuranyl (THF)[12] or tetrahydropyranyl (THP)[13] protecting groups on the synthetic yields of the subsequent steps of the synthetic sequence. Although the spin trapping properties of the final product, HMMPO, must be expected to be not optimal for superoxide radicals, utilization of those protecting groups in combination with the pyrrolidine *N*-oxide moiety seems to offer a valuable and versatile building block for later modification with a series of different targeting groups, for example, towards cationic spin traps which have a specific selectivity for mitochondria.

2. Results

2.1. Structure of the spin traps

The spin traps reported within this study are derived from the commercially available parent compound 5,5-dimethyl-1-pyrroline-*N*-oxide (DMPO), to which an additional hydroxyl substituent (unprotected or protected by a THF or THP group) had been introduced to one of the methyl groups in position 5. This led to 5-hydroxymethyl-5-methyl-1-pyrroline-*N*-oxide (HMMPO), 5-(2-furanyloxymethyl)-5-methyl-1-pyrroline-*N*-oxide (FMMPO), and 5-(2-pyranyloxymethyl)-5-methyl-1-pyrroline-*N*-oxide (PMMPO). The structures are shown in Figure 1a, the synthetic steps in Figure 1b, and the spectroscopic data are summarized in Tables 1–6 (NMR, MS, IR, UV–vis and EPR parameters).

The structural identity of the novel spin traps was confirmed by ^{13}C NMR (Table 1), ^{1}H NMR (Table 2), MS and microanalysis

* Corresponding author. Tel.: +43 1 25077 4406; fax: +43 1 25077 4490.
E-mail address: klaus.stolze@vetmeduni.ac.at (K. Stolze).

0968-0896/$ - see front matter © 2010 Elsevier Ltd. All rights reserved.
doi:10.1016/j.bmc.2010.11.052

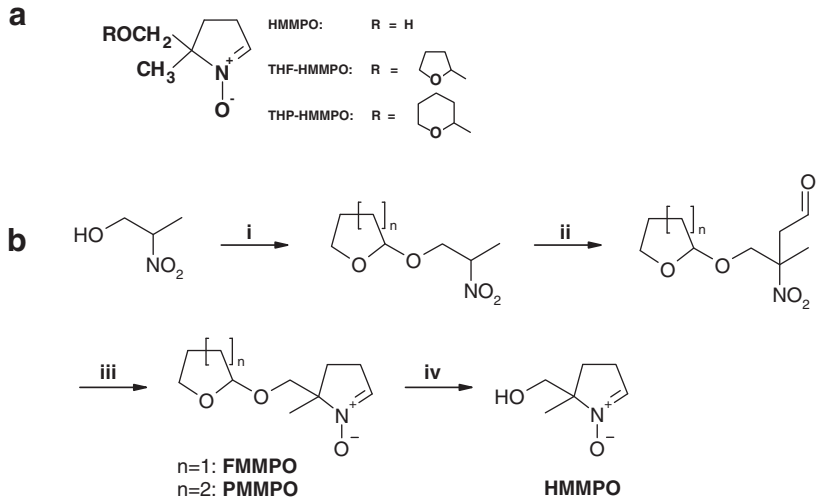

i: 2,3-dihydrofurane (or 3,4-dihydro-(2*H*)-pyrane), H^+; **ii**: H_2C=CH-CHO, MeCN, NEt_3; **iii**: NH_4Cl / Zn, H_2O/MeOH (v/v=6:4); **iv**: HCl

Figure 1. (a) General structure of the spin traps and (b) general synthetic scheme.

Table 1
^{13}C NMR data [ppm] of the spin traps

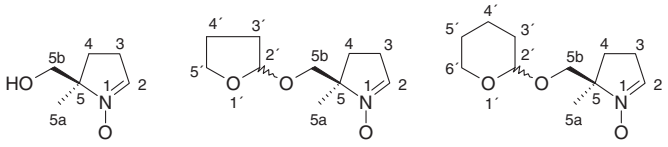

	^{2}C	^{3}C	^{4}C	^{5}C	^{5a}C	^{5b}C	$^{2'}C$	$^{3'}C$	$^{4'}C$	$^{5'}C$	$^{6'}C$
EMPO[3]	134.9	25.4	31.9	78.5	20.3	169.3 (C=O)	61.7 (CH_2)	13.4 (CH_3)	–	–	–
HMMPO	137.5	25.3	28.3	76.5	20.5	66.0	–	–	–	–	–
FMMPO	134.7 & 135.2	25.3 & 25.4	29.2 & 29.6	76.1 & 76.4	21.5 &21.6	69.7 & 69.9	103.9 &104.1	23.3 & 23.5	32.4	67.1	–
PMMPO	134.1 & 134.7	25.55 & 25.6	29.6 & 29.9	76.2 & 76.5	21.7 & 21.8	70.2 & 70.9	98.2 & 99.7	30.6 & 30.8	19.1 & 20.0	25.62	61.6 & 63.0

Table 2
^{1}H NMR data [ppm] of the spin traps

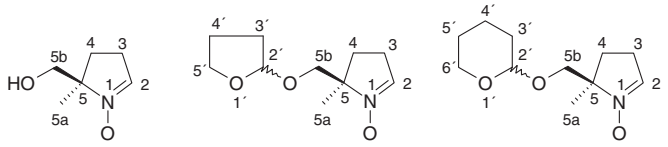

	^{2}CH	$^{3}CH_2$	$^{4}CH_2$	$^{5a}CH_3$	$^{5B}CH_3$	$^{2'}CH$	$^{3'}CH_2$	$^{4'}CH_2$	$^{5'}CH_2$	$^{6'}CH_2$	OH
EMPO[3]	6.97 t	2.75 m	2.16 m 2.60 m	1.72 s	–	4.26 m (CH_2)	1.31 t (CH_3)	–	–	–	–
HMMPO	7.04 s	2.55–2.72 m	1.92–2.02 m 2.40–2.49 m	1.38 s	3.43 d 3.93 d	–	–	–	–	–	4.50 s, br
FMMPO	6.92 s 6.95 s	2.51–2.60 m	1.95–2.03 m 2.40–2.48 m	1.36 s & 1.38 s	3.23 d 3.49 d 3.87 d 4.04 d	5.13 m	1.75–1.87 m 1.90–1.96 m	1.83–1.88 m	3.83–3.92 m	–	–
PMMPO	6.90 s	2.57–2.70 m	1.96–2.06 m 2.47–2.56 m	1.38 s & 1.41 s	3.20 d 3.60 d 3.85 d 4.15 d	4.15 m	1.45–1.63 m	1.64–1.79 m	1.45–1.63 m 3.83–3.92 m	3.48–3.56 m 3.79–3.88 m	

Table 3
MS/microanalysis of the spin traps

	$[MH]^+$	Calcd $[MH]^+$	C calcd	C found	H calcd	H found	N calcd	N found
HMMPO	130.17	130.17	55.80	55.72	8.58	8.72	10.84	10.88
FMMPO	200.26	200.26	60.28	60.19	8.60	8.73	7.03	6.98
PMMPO	214.28	214.29	61.95	61.88	8.98	9.17	6.57	6.39

Table 4
IR data (cm^{-1}) of the spin traps[4]

EMPO[a]	**2985**	**2940**	2874	**1741**	**1582**	**1464**	**1446**	**1377**	1341	**1288**	**1236**	**1182**	–	**1107**	–	–	1024	–	950	926	**862**	796	–	–
DMPO	**3086**	**2974**	**2933**	**2872**	1662	**1583**	**1458**	**1367**	**1344**	**1271**	**1232**	**1144**	**1117**	1026	935	824	779	**714**	**690**	**635**	**584**	**507**		
HMMPO	**3307**	**2980**	**2927**	**2902**	**2872**	1670	**1597**	**1541**	**1456**	1383	1346	1294	**1215**	**1196**	1124	**1065**	1024	976	945	**779**	**725**	**698**	**652**	**586**	500
FMMPO	**2980**	**2949**	**2879**	1659	**1589**	**1458**	1375	1346	1296	**1225**	**1196**	**1101**	**1047**	**970**	**945**	**920**	860	781	696	654	592	509		
PMMPO	**2947**	**2916**	**2872**	**2850**	1651	**1585**	**1456**	1377	1348	1323	**1228**	**1200**	**1124**	**1070**	**1036**	**974**	**905**	870	814	779	694	646	594	560	500

Intensities: **strong (1741)**, **medium (1464)**, weak (950).
[a] Data from Stolze et al. (2003).[4]

Table 5
Half-life of the superoxide adducts, *n*-octanol/buffer partition coefficients, and UV–vis spectroscopic data of the spin traps

Compound	Apparent $t_{1/2}$ (min)	partition coefficient *n*-octanol/ phosphate buffer (100 mM, pH 7.0)	UV data λ_{max} and molar absorptivity ε ($l\ mol^{-1}\ cm^{-1}$)
DMPO	0.835 (–)1 0.91 (α-CD) 1.53 (β-CD) 0.75 (γ-CD) 1.65 (2,6-DM-β-CD)	0.13	–
EMPO	8.6 (–)[3] 17.8 (α-CD) 53.3 (β-CD) 26.1 (γ-CD) 66.1 (2,6-DM-β-CD)	0.15	231 nm, 7417 ± 46
HMMPO	3.53 (–) 4.71 (α-CD) 7.82 (β-CD) 4.02 (γ-CD) 4.42 (2,6-DM-β-CD)	0.041 ± 0.001	228 nm, 6123 ± 54
FMMPO	3.43 (–) 3.72 (α-CD) 4.70 (β-CD) 4.57 (γ-CD) 5.76 (2,6-DM-β-CD)	0.347 ± 0.006	228 nm, 7015±46
PMMPO	4.76 (–) 4.42 (α-CD) 6.03 (β-CD) 5.08 (γ-CD) 6.73 (2,6-DM-β-CD)	0.845 ± 0.002	228 nm, 6666 ± 26

(Table 3), FT-IR spectroscopy (Table 4) and UV–vis spectroscopy (Table 5).

A complete set of ^1H, H–H correlated, ^{13}C, HMQC and HMBC spectra was recorded for each compound, which allowed for a complete signal assignment in both the ^1H and ^{13}C domains.

^{13}C NMR confirmed the presence of a heterocyclic pyrroline ring. The resonances for C-2 were found between 134.1 and 137.5 ppm, comparable to EMPO and its derivatives (around 134.9 ppm). The C-3 resonances (signal at about 25 ppm) were also comparable to EMPO. A slight upfield shift by about 2 ppm was seen for the neighboring C-4 (approx. 28–30 ppm, vs 31.9 ppm for EMPO), and for C-5 (approx. 76.1–76.5 ppm, vs 78.5 ppm for EMPO). The 5a-substituent, resonating at 20.3 ppm in EMPO, was shifted downfield by about 1 ppm, being found around 22 ppm for the derivatives described herein. The carboxylic carbon in EMPO (resonating at 169.3 ppm) was replaced by a 5b-hydroxymethyl group in HMMPO (66 ppm), and 5b-alkoxymethyl groups in FMMPO and PMMPO (approx. 70 ppm). The resonances of the 2-furanyl and 2-pyranyl protecting groups agree with the expectations.

The proton spectra showed some interesting features. H-2 (around 7 ppm) appeared as a singlet, in contrast to EMPO and most of its derivatives, for which the expected triplet was found that indicated similar coupling constants to the geminal H-3 protons. The observed singlet indicates that the coupling constants to both H-3 are close to zero.

The resonance of the 4-methylene and the 5b-oxymethylene group show a strong enantiotopic/diastereotopic splitting of about 0.5 ppm.

The major absorption peaks in the respective FT-IR spectra were seen around 1580 cm^{-1} (C=N) and 1205 cm^{-1} (N–O).

2.2. Superoxide radical adducts

Previously reported methods for the generation of superoxide adducts were applied in our study.[2–7,18,19] However, the low stabil-

ity of superoxide adducts of HMMPO, FMMPO, and PMMPO rendered the detection of the expected ESR signal rather difficult. In addition, several secondary products were also formed, one of them being the hydroxyl radical adduct also seen in the case of commercially available DMPO. Half-lives of the superoxide spin adducts showed no significant advantage over the spin trap DMPO. In order to increase the stability we decided to employ the formation of stable cyclodextrin complexes which has recently been reported by several groups.[14–17] Since it was not known which of the commercially available cyclodextrins and cyclodextrin derivatives would be best suitable for spin adduct stabilization, a set of 4 compounds, namely α-, β-, γ-cyclodextrin, and heptakis-(2,6-di-*O*-methyl)-β-cyclodextrin, was tested. The stabilizing effects of the different cyclodextrins are shown in Figs. 2–4. For comparison, also cucurbit[6]uril, a cavitand build of methylene-bridged glycoluril

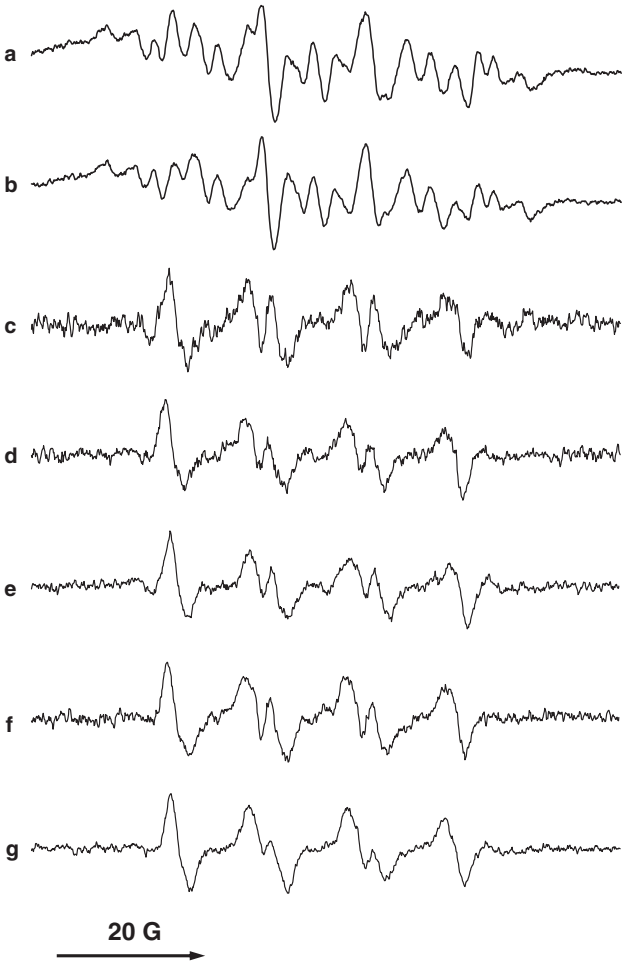

Figure 2. Superoxide radical spin adducts formed from HMMPO in a hypoxanthine/xanthine oxidase system stabilized by different cyclodextrin derivatives. HMMPO (8 mM) was dissolved in oxygenated phosphate buffer (100 mM, pH 7.4, containing 0.4 mM DTPA), catalase (250 U/mL), hypoxanthine (0.2 mM) and xanthine oxidase (500 mU/mL). After 15 min incubation maximum intensity was reached, SOD (150 units/mL) was added and a series of consecutive ESR spectra (every 90 s for 30 min) was recorded using the following EPR parameters: sweep width, 80 G; modulation amplitude, 1.17 G; microwave power, 20 mW; time constant, 0.16 s; receiver gain, 2×10^5; scan rate, 57 G/min. (a) Scans accumulated from 0 to 6 min after mixing (relative intensity: 47). (b) Scans accumulated from 7.5 to 15 min (rel. int.: 60). (c) Difference spectrum: Fig. 2a—0.9 × Fig. 2b (rel. int.: 18). Under otherwise identical conditions as in (a), the following cyclodextrins were added: (d) + α-Cyclodextrin (16 mM, rel. int.: 25). (e) + β-Cyclodextrin (16 mM, rel. int.: 32). (f) + γ-Cyclodextrin (16 mM, rel. int.: 27). (g) + Heptakis-(di-*O*-methyl-)-β-cyclodextrin (16 mM, rel. int.: 41).

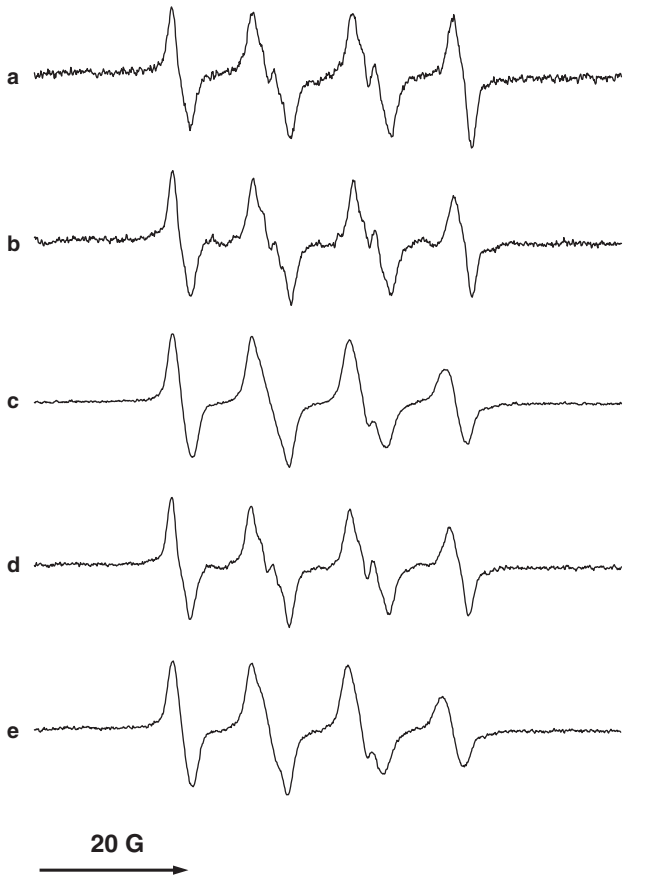

Figure 3. Superoxide radical spin adducts formed from FMMPO in a hypoxanthine/xanthine oxidase system stabilized by different cyclodextrin derivatives. FMMPO (8 mM) was dissolved in oxygenated phosphate buffer (100 mM, pH 7.4, containing 0.4 mM DTPA), catalase (250 U/mL), hypoxanthine (0.2 mM) and xanthine oxidase (500 mU/mL). (a) Without cyclodextrin added (rel. int.: 21), (b) α-cyclodextrin (16 mM, rel. int.: 29), (c) β-cyclodextrin (16 mM, rel. int.: 70), (d) γ-cyclodextrin (16 mM, rel. int.: 43), (e) heptakis-(di-*O*-methyl-)-β-cyclodextrin (16 mM, rel. int.: 55). After 15 min incubation maximum intensity was reached. SOD (150 units/mL) was added and a series of consecutive ESR spectra (every 90 s for 30 min) was recorded using the following EPR parameters: sweep width, 80 G; modulation amplitude, 0.83 G; microwave power, 20 mW; time constant, 0.08 s; receiver gain, 2×10^5; scan rate, 57 G/min.

units, was tested, but did not lead to a stabilization of any of the investigated superoxide adducts (spectra not shown).

Superoxide radicals were generated using a hypoxanthine (0.2 mM)/xanthine oxidase (500 mU/ml) system in the presence of the spin trap (8 mM) and a 2-fold excess of the respective cyclodextrin (16 mM) in 10 mM oxygenated phosphate buffer pH 7.4, containing 1 mM DTPA. When the maximum ESR intensity was obtained (ranging from ca. 1 min for DMPO to 15 min for EMPO) SOD (ca. 150 U/ml) and catalase (250 U/mL) were added to stop superoxide production. Decay kinetics of the superoxide adducts were calculated as follows: A series of repetitive scans was recorded for each incubation (every 45 s over 15 min for DMPO, every 90 s over 30 min for the other compounds) using a first-order exponential decay approximation (Table 5, Pearson correlation coefficient $R^2 > 0.99$).

The resulting ESR spectra obtained with 8 mM HMMPO alone (no cyclodextrin added) are shown in Figure 2a (five scans accumulated from 0 to 6 min after mixing) and in Figure 2b (recorded from 7.5 to 15 min after mixing). Both ESR spectra show a mixture of several paramagnetic species with variable intensities. The EPR lines of the rapidly decaying HMMPO/$^{\cdot}$OOH spin adduct became visible only in the form of a difference spectrum (Fig. 2c, corre-

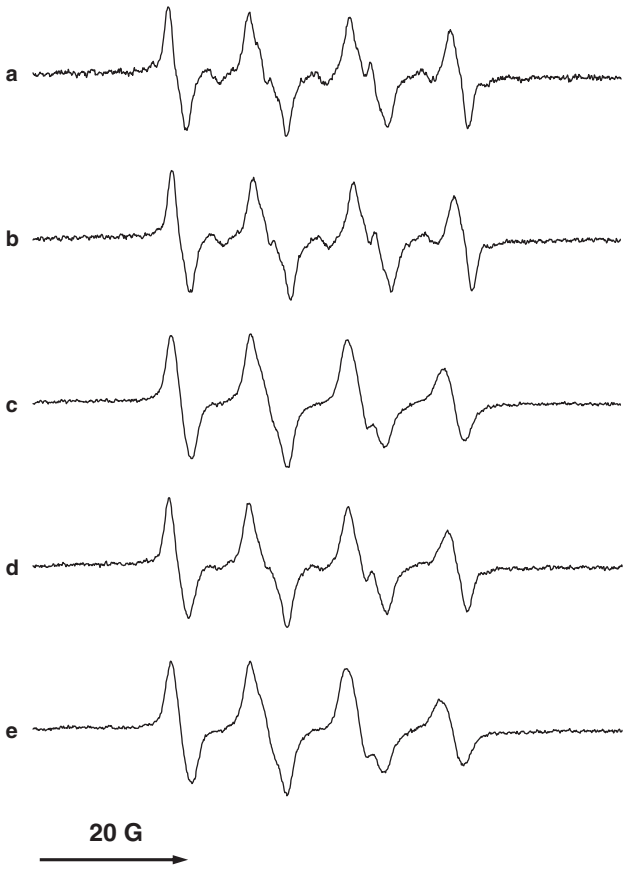

Figure 4. Superoxide radical spin adducts formed from PMMPO in a hypoxanthine/xanthine oxidase system stabilized by different cyclodextrin derivatives. PMMPO (8 mM) was dissolved in oxygenated phosphate buffer (100 mM, pH 7.4, containing 0.4 mM DTPA), catalase (250 U/mL), hypoxanthine (0.2 mM) and xanthine oxidase (500 mU/mL). (a) Without cyclodextrin added (relative intensity: 29), (b) α-cyclodextrin (16 mM, rel. int.: 35), (c) β-cyclodextrin (16 mM, rel. int.: 55), (d) γ-cyclodextrin (16 mM, rel. int.: 43), (e) heptakis-(di-*O*-methyl-)-β-cyclodextrin (16 mM, rel. int.: 50). After 15 min incubation maximum intensity was reached. SOD (150 units/mL) was added and a series of consecutive ESR spectra (every 90 s for 30 min) was recorded using the following EPR parameters: sweep width, 80 G; modulation amplitude, 0.83 G; microwave power, 20 mW; time constant, 0.08 s; receiver gain, 2×10^5; scan rate, 57 G/min.

sponding to **2a**—0.9 × 2b), indicating that the intensity of the secondary products changed only gradually during the first 15 min.

The respective EPR spectra recorded in the presence of 16 mM α-cyclodextrin (Fig. 2d), 16 mM β-cyclodextrin (Fig. 2e), 16 mM γ-cyclodextrin (Fig. 2f), and 16 mM heptakis-(2,6-di-*O*-methyl)-β-cyclodextrin (Fig. 2g) were obtained in the same way, as difference spectra as discussed above (Fig. 2c). The shape of the ESR spectra strongly varies with the complexing agent used. Due to the low stability of the non-complexed superoxide adducts and the limited solubility of β-cyclodextrin in buffer, concentration-dependent studies of superoxide half lives and HFS parameters were not possible. Therefore, a constant 2:1 ratio between the spin trap and the cyclodextrin was chosen, the concentration of cyclodextrin being 16 mM, which was the highest concentration of β-cyclodextrin in aqueous buffer achievable.

The stability of the superoxide adducts of FMMPO and PMMPO (Figs. 3 and 4) were significantly higher than those with HMMPO, the EPR spectra could therefore be detected directly, without calculation of difference spectra. All experiments were performed with 8 mM of FMPPO with no cyclodextrin added (Fig. 3a), and with 16 mM of α-cyclodextrin (Fig 3b), β-cyclodextrin (Fig. 3c), γ-cyclodextrin (Fig. 3d), and heptakis-(2,6-di-*O*-methyl)-β-cyclodextrin (Fig. 3e), respectively.

The superoxide adducts obtained with PMPPO (8 mM) are shown in Figure 4a–e (without cyclodextrin, and with 16 mM of α-cyclodextrin, β-cyclodextrin, γ-cyclodextrin, and heptakis-(2,6-di-*O*-methyl)-β-cyclodextrin, respectively). The relative intensities of the EPR spectra are listed in the figure legends.

2.3. Hydroxyl radical adducts

In order to form the respective hydroxyl radical adducts, the spin traps (40 mM) were incubated with an aqueous Fenton system[20,21] (H_2O_2 (0.2%), EDTA (2 mM), and iron(II) sulfate (1 mM)). After 10 s the reaction mixture was diluted 1:1 with phosphate buffer (300 mM, pH 7.4; 20 mM DTPA), and the EPR spectra were recorded immediately (Fig. 5). Only one major compound was found for HMMPO/·OH (Fig. 5a), whereas two different species were detected with FMMPO/·OH (ratio 58%/42%; Fig. 5b) and PMMPO/·OH (ratio 64%/36%; Fig. 5c). The secondary species is a carbon-centered radical of unknown structure, most probably derived from degradation of the spin trap or spin adduct. The respective HFS data, obtained by computer simulation, are listed in Table 6.

2.4. Methyl radical adducts

In analogy to our previous investigations with EMPO derivatives,[3–7] we synthesized the respective methyl radical adducts using an aqueous Fenton system in the presence of 10% DMSO.[20] Also here the reaction mixture was diluted 1:1 with phosphate

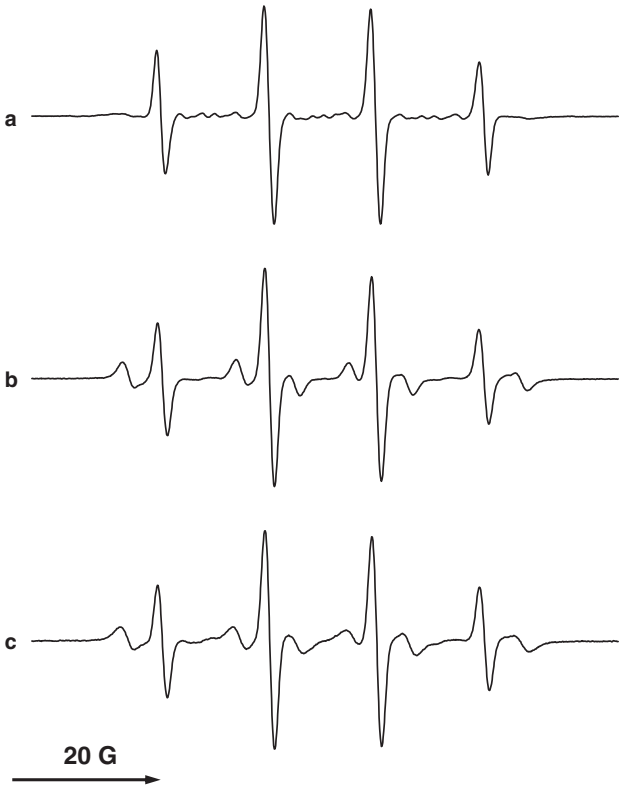

Figure 5. Iron-dependent formation of hydroxyl radical spin adducts from HMMPO, FMMPO, and PMMPO. (a) HMMPO (40 mM, initial concentration) was incubated with a Fenton system containing $FeSO_4$ (1 mM), EDTA (2 mM), H_2O_2 (0.2%). The reaction was stopped after 10 s by 1:1 dilution with phosphate buffer (300 mM, pH 7.4, containing 20 mM DTPA) and the spectrum was recorded using the following spectrometer settings: sweep width, 80 G; modulation amplitude, 0.21 G; microwave power, 20 mW; time constant, 0.08 s; receiver gain, 1×10^4; scan rate, 57 G/min (rel. int.: 45), (b) same as in (a), except that FMMPO was used (rel. int.: 33), (c) same as in (a), except that PMMPO was used (gain 2.5×10^4, rel. int.: 37).

Table 6
Comparison of the EPR parameters of radical adducts of EMPO, DMPO, HMMPO, FMMPO, and PMMPO.

Radical	HFS (G)	EMPO[a]		DMPO		HMMPO		FMMPO		PMMPO	
		trans[b]	cis[b]								
·OOH	(−)	(94%)[c]	(6%)	(100%)		(62%)	(38%)	(35%)	(65%)	(45%)	(55%)
	a^N	13.27 13.25	13.25	14.30		13.55	13.70	13.69	13.68	13.73	13.75
	a^H	12.37 9.30	10.15	11.70		12.17	10.23	12.60	10.15	12.73	13.75
	a^H	(55.5%/44.5% of of trans[c])	1.50	1.25		0.55	1.00	–	(0.80)	0.55	0.80
·OOH	(α-CD)	(38%)	(62%)	(54%)	(46%)	(34%)	(66%)	(35%)	(65%)	(49%)	(51%)
	a^N	13.22	13.22	14.15	14.15	15.15	14.49	13.70	13.70	13.73	13.73
	a^H	11.90	9.66	12.55	10.05	12.31	10.20	12.60	10.18	12.40	9.89
	a^H	–	–	–	–	0.55	1.00	–	0.80	0.55	0.70
OOH	(β-CD)	(61%)	(39%)	(50%)	(50%)	(52%)	(48%)	(53%)	(47%)	(59%)	(41%)
	a^N	12.73	12.73	13.57	13.58	13.65	13.60	13.35	13.30	13.10	13.10
	a^H	12.00	9.82	12.27	9.84	12.00	9.70	12.10	9.55	11.80	9.05
	a^H	–	–	–	–	0.55	0.70	(0.55)	(0.70)	0.55	0.70
·OOH	(2,6-DMBCD)	(50%)	(50%)	(48%)	(52%)	(44%)	(56%)	(27%)	(73%)	(42%)	(58%)
	a^N	12.56	12.56	13.50	13.52	13.30	13.26	13.00	13.10	13.05	12.90
	a^H	11.95	9.75	12.40	9.95	12.27	9.74	12.35	9.50	11.95	9.65
	a^H	–	–	–	–	0.55	0.95	0.85	0.90	0.55	0.90
·OOH	(γ-CD)	(55%)	(45%)	(53%)	(47%)	(40%)	(60%)	(32%)	(68%)	(32%)	(68%)
	a^N	13.16	13.17	14.06	14.02	13.54	13.55	13.50	13.55	13.20	13.57
	a^H	11.81	9.51	12.48	10.10	12.25	9.95	12.60	10.04	12.60	10.35
	a^H	–	–	–	–	0.55	0.93	–	1.00	0.55	1.15
		EMPO		DMPO		HMMPO		FMMPO		PMMPO	
		trans[b]	cis[b]								
·OH		(76%)	(24%)	(100%)		(100%)		(58%)	(42%)[f]	(64%)	(36%)[f]
	a^N	14.11	14.18	14.80		14.44		14.60	15.46	14.62	15.49
	a^H	12.80	15.27	14.80		14.98		14.67	22.67	14.73	22.85
	a^H	0.63	0.62								
	a^H	0.43	0.50								
	a^H	$0.21^{(3)}$	$0.29^{(3)}$								
	a^H	$0.13^{(2)}$	$0.07^{(2)}$								
·H	a^N	(100%)		(100%)		(100%)		(100%)		(100%)	
	a^N	15.52		16.00		16.00		16.00		16.00	
	a^H	22.21		21.50		21.20		21.40		21.31	
	a^H	20.82		21.50		22.85		22.70		22.80	
·CH_3		(100%)		(100%)		(100%)		(100%)		(100%)	
	a^N	15.42		16.56		15.79		15.83		15.76	
	a^H	22.30		23.68		23.52		23.30		23.46	
	a^H	–	–								
·OCH_3		(50%)	(50%))	(100%)		–		(100%)[e]		(100%)[e]	
	a^N	13.74	13.74	13.58		–		14.1		14.0	
	a^H	10.87	7.81	7.61		–		9.9		10.1	
	a^H	–	–	1.85 (organic solvent)		–		1.4		1.4	
·CH_2OH		(100%)		(100%)		(100%)		(100%)		(100%)	
	a^N	14.95		16.20		15.36		15.38		15.39	
	a^H	21.25		23.00		22.40		22.00		22.07	
	a^H	–		–		–		–		–	
·$CH(OH)CH_3$		(67%)	(33%)	(100%)		(100%)		(100%)		(100%)	
	a^N	14.94	15.00	16.00		15.33		15.39		15.40	
	a^H	20.82	22.40	23.00		22.87		22.57		22.55	
·CO_2^-		(100%)		(100%)		(70%)	(30%)	(58%)	(42%)	(90%)	(10%)
	a^N	14.74		15.80		15.15	14.49	15.18	14.61	15.22	14.64
	a^H	17.16		18.80		19.02	14.94	18.70	14.61	18.78	14.64
	–	–				–	0.50	–	0.60	–	0.60

[a] Data from Stolze et al.[3,7], except for b and c.
[b] Data from Culcasi et al.[24]
[c] Mixture of rotamers.
[d] Approximate values, obtained from difference spectra.
[e] Carbon-centered radical adduct.

buffer (300 mM, pH 7.4; 20 mM DTPA) after brief incubation. Due to the high line width the respective EPR spectra showed the presence of only one major component of HMMPO/·CH_3 (Fig. 6a), PMMPO/·CH_3 (Fig. 6b) and PMMPO/·CH_3 (Fig. 6c).

2.5. Methanol and ethanol-derived radical adducts

The above-mentioned Fenton-type incubation system[20,21] was used, except that methanol or ethanol was used instead of DMSO. The EPR spectra of the ·CH_2OH radical adducts of HMMPO, FMMPO, and PMMPO can be seen in Figure 7a–c, respectively. EPR parameters for the ·$CH(CH_3)OH$ radical adducts are listed in Table 6. Due to the presence of more than one chiral center, different diastereomeric forms of the spin adducts can be expected. Because of the high line width these diasteromeric forms can, however, not be resolved. The lines of low intensity in between most probably are traces of the respective hydroxyl and methoxyl radical adducts.

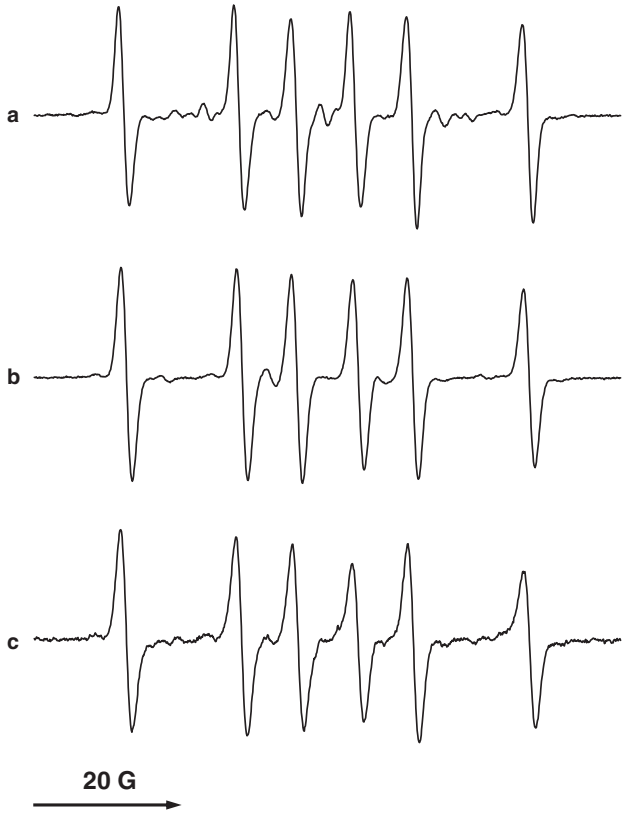

Figure 6. *Iron-dependent formation of methyl radical spin adducts from HMMPO, FMMPO, and PMMPO in the presence of DMSO.* (a) HMMPO (40 mM, initial concentration) was incubated with a Fenton system containing $FeSO_4$ (1 mM), EDTA (2 mM), H_2O_2 (0.2%) in 20% DMSO. The reaction was stopped after 10 s by 1:1 dilution with phosphate buffer (300 mM, pH 7.4, containing 20 mM DTPA) and the spectrum was recorded using the following spectrometer settings: sweep width, 80 G; modulation amplitude, 0.21 G; microwave power, 20 mW; time constant, 0.08 s; receiver gain, 1×10^4; scan rate, 57 G/min (rel. int.: 11), (b) same as in (a), except that FMMPO was used (rel. int.: 12), (c) same as in (a), except that PMMPO was used (gain 2.5×10^4, rel. int.: 9).

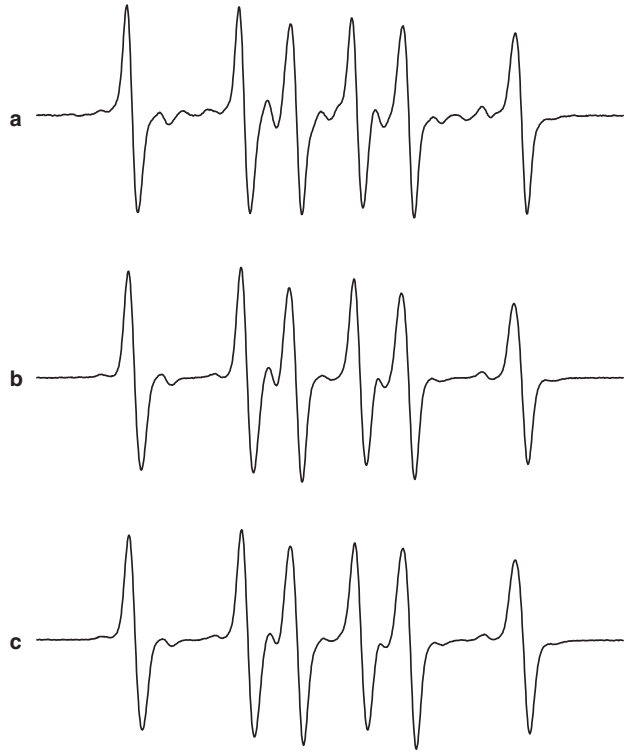

Figure 7. Iron-dependent formation of hydroxymethyl radical spin adducts from HMMPO, FMMPO, and PMMPO in the presence of methanol. (a) HMMPO (40 mM, initial concentration) was incubated with a Fenton system containing $FeSO_4$ (1 mM), EDTA (2 mM), H_2O_2 (0.2%) in 20% methanol. The reaction was stopped after 10 s by 1:1 dilution with phosphate buffer (300 mM, pH 7.4, containing 20 mM DTPA) and the spectrum was recorded using the following spectrometer settings: sweep width, 80 G; modulation amplitude, 0.21 G; microwave power, 20 mW; time constant, 0.08 s; receiver gain, 1×10^4; scan rate, 57 G/min (rel. int.: 19), (b) same as in (a), except that FMMPO was used (rel. int.: 22), (c) same as in (a), except that PMMPO was used (gain 2.5×10^4, rel. int.: 52).

2.6. Other spin adducts formed

Similarly, the use of an aqueous sodium formate solution (200 mM) under otherwise identical conditions lead to the formation of the respective carbon dioxide anion radical adducts.[20,21] The characteristic ESR spectra are shown in Figure 8a (HMMPO/$^{\cdot}CO_2^-$), Figure 8b (FMMPO/$^{\cdot}CO_2^-$), and Fig. 8c (PMMPO/$^{\cdot}CO_2^-$). Two clearly different diastereomeric forms could be distinguished with all spin traps. The HFS data are listed in Table 6. We also tried to synthesize the respective methoxyl radical adducts according to a procedure previously published by Dikalov et al.[22] In our previous studies using a series of EMPO derivatives,[3–7] transient $\cdot OCH_3$ adducts could be detected from most of the spin traps investigated. With HMMPO only the hydroxymethyl adduct (see above, Fig. 7) was seen, FMMPO and PMMPO formed the respective hydroxymethyl adduct as the major species with traces of a very short lived methoxyl radical adduct, detectable only as poorly resolved difference spectra (not shown). Approximate HFS constants have been calculated and added to Table 6.

Reduction of spin traps with KBH_4 usually leads to the formation of pseudo-H$^{\cdot}$ adducts. This was also confirmed for the three new spin traps in the present study: Addition of a small amount of KBH_4 (ca. 0.5 mg/500 μl) to the respective spin trap (40 mM), followed by readjusting of the pH to 7.4 by 1:1 dilution with phosphate buffer (300 mM, pH 7.4, containing 20 mM DTPA) led to the observation of the respective H$^{\cdot}$ adducts with all three compounds (spectra not shown, EPR parameters listed in Table 6).

3. Discussion

Three novel spin traps that can be regarded as DMPO derivatives with a hydroxymethyl or alkoxymethyl group in position 5 of the pyrroline ring were synthesized in this study and were compared with the parent compound DMPO as well as with similar spin traps, such as EMPO and its derivatives.[3–7] The chemical structure and purity of all compounds was comprehensively supported by full NMR assignment (^1H and ^{13}C), MS, microanalysis, FT-IR, and UV–vis spectroscopy (Tables 1–5).

The presence of functional groups in spin traps, such as hydroxyl or amino functionalities, allows for structural modification under mild conditions so as to direct the spin trap to specific areas or organells. The presence of two chiral carbon centers leads to the formation of two different diastereomers of the investigated spin traps. Addition of radicals from two different sides eventually leads to four different stereoisomers, which have similar EPR parameters and can, therefore, not always be clearly distinguished. In addition, formation of secondary products due to side reactions and degradation of spin adducts complicates the situation even further.

Unfortunately, the stabilities of the respective superoxide adducts are rather low, that is, similar to the parent compound DMPO or slightly higher, but significantly lower than the structurally related EMPO derivatives. On the other hand, previous studies with hydroxyl-substituted DEPMPO compounds revealed higher

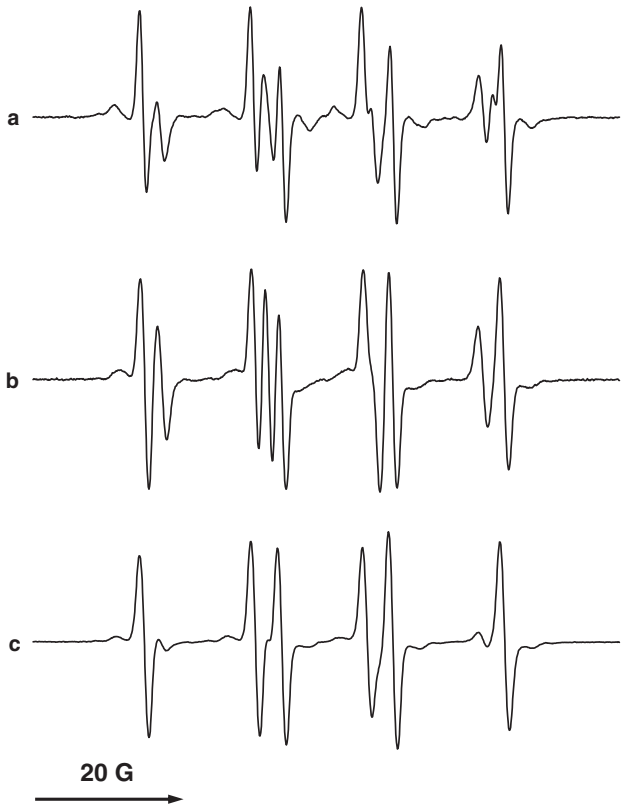

Figure 8. *Iron-dependent formation of carbon-centered spin adducts from HMMPO, FMMPO, and PMMPO in the presence of formate* (a) HMMPO (40 mM, initial concentration) was incubated with a Fenton system containing $FeSO_4$ (1 mM), EDTA (2 mM), H_2O_2 (0.2%) and sodium formate (200 mM). The reaction was stopped after 10 s by 1:1 dilution with phosphate buffer (300 mM, pH 7.4, containing 20 mM DTPA) and the spectrum was recorded using the following spectrometer settings: sweep width, 80 G; modulation amplitude, 0.21 G; microwave power, 20 mW; time constant, 0.08 s; receiver gain, 1×10^4; scan rate, 57 G/min (rel. int.: 15), (b) same as in (a), except that FMMPO was used (rel. int.: 13), (c) same as in (a), except that PMMPO was used (gain 2.5×10^4, rel. int.: 65).

superoxide adduct stabilities,[8–10] although the reported synthetic procedure is rather complex. In view of the low stabilities of the superoxide adducts we investigated the stabilizing effect of β-cyclodextrin and compared it to the values obtained with DMPO and EMPO. Replacement of β-cyclodextrin by α-, γ-, or heptakis-(2,6-di-*O*-methyl)-β-cyclodextrin gave considerably different results, the use of cucurbit[6]uril (spectra not shown) did not show any stabilizing effect at all.

All spin traps are forming characteristic hydroxyl radical adducts: Methoxyl radical adducts were rather unstable and could only be detected from FMMPO and PMMPO as minor components in mixtures with the predominant hydroxymethyl radical adduct. From two EPR spectra recorded at different time intervals poorly resolved spectra of the FMMPO and PMMPO methoxyl radical adducts could be calculated, whereas from HMMPO no methoxyl radical adduct was detectable under these conditions. The most stable spin adducts were formed from carbon-centered radicals, for example, from DMSO ($\cdot CH_3$), methanol ($\cdot CH_2OH$), ethanol ($\cdot CH(CH_3)OH$), and formate ($\cdot CO_2^-$).

4. Conclusion

In conclusion, all three novel DMPO-derived spin traps formed rather unstable superoxide adducts ($t_{1/2}$ ca. 3–5 min) and can therefore not be recommended for superoxide trapping, although cyclodextrins showed a significant stabilizing effect on the radical adducts in all cases. In contrast to this, stable carbon-centered radical adducts are formed from all investigated spin traps. The prospect of facile modification of the novel compounds under mild conditions justifies further research with respect to better yields and higher adduct stabilities.

5. Experimental

5.1. Chemicals

Acrolein and triethylamine were commercially available from Fluka, 2-nitropropanol, 2,3-dihydrofurane, and 3,4-dihydro-(2*H*)-pyrane were from Sigma–Aldrich, all other chemicals were obtained from VWR.

5.2. Syntheses

Synthesis and characterization of the compounds were performed in analogy to those reported previously for the synthesis of derivatives of EMPO[3–7,18,23] with modifications as given below.

5.2.1. 2-Nitropropanol tetrahydrofuranyl and tetrahydropyranyl ether

To 7 ml of 2-nitropropanol (8.3 g; 78.9 mmol) either 1 ml of 2,3-dihydrofurane (0.927 g; 13.07 mmol for the tetrahydrofuranyl ether) or 1 ml of 3,4-dihydro(2*H*) pyrane (0.93 g; 11.05 mmol, for the tetrahydropyranyl ether) was added. HPLC (75% methanol in water as the eluent on a 250 × 4.6 mm C-18 column) was run as a control. Toluenesulfonic (10 mg) acid was added as a catalyst and the reaction was monitored every 15 min by HPLC. One milliliter of portions of either 2,3-dihydrofurane (THF ether) or 3,4-dihydro-(2*H*)-pyrane (THP ether) were added at 10 min intervals, until the HPLC runs confirmed that the reaction was complete (after ca. 1 h and a total amount of 7 ml of 2,3-dihydrofurane or 8 ml of 3,4-dihydro-(2*H*)-pyrane added). Average yield: 94% of crude product, which was used without further purification.

5.2.2. 2-(2-Furanyl)-oxy-2-nitropentanal and 2-(2-pyranyl)-oxy-2-nitropentanal

The crude product of the respective tetrahydrofuranyl ether (73.6 mmol; 13 g) or tetrahydropyranyl ether (73.6 mmol; 14 g) was dissolved in 50 ml acetonitrile at 0 °C and 2 ml of triethylamine was added. Acrolein (6 ml; 88.8 mmol) was slowly added in 1 ml portions while the reaction was monitored by HPLC (75% methanol; 250 × 4.6 mm C-18). After 30 min the ice bath was removed und the reaction mixture was stirred at room temperature until the reaction was complete (after ca. 2 h). The solvent and the triethylamine were removed at reduced pressure and the purity of the crude product (ca. 95% yield) was assessed by HPLC. The product was used without further purification.

5.2.3. Synthesis of the nitrones

Synthesis of the nitrones was performed in analogy to previously published EMPO derivatives[3–7] with the following modifications:

Ca. 70 mmol of the crude 2-(2-furanyl)-oxy-2-nitropentanal (or 2-(2-pyranyl)-oxy-2-nitropentanal) was dissolved in 40 ml of methanol and a solution of 3 g NH_4Cl in 60 ml water was added which causes a partial precipitation of the solutes. Zn (11 g) powder (168 mmol) was gradually added in steps of 1 g under HPLC control (dissolution of 20 μl of the mixture in 1 ml of methanol in an Eppendorf tube and centrifugation for 1 min). After 1 h, acetic acid was carefully added in small amounts (ca. 200 μl) until the product peak in the HPLC control had passed its maximum. The

solution was filtered and washed three times with 30 ml methanol. The filtrate was extracted 5 times with 100 ml of organic solvent (75% petroleum ether/25% methylene chloride) in order to remove unreacted starting material (the respective pentanal). The organic phase was extracted 5 times with 30 ml water and was discarded afterwards. The original filtrate (containing the Zn salts) was extracted five times with 50 ml of methylene chloride. The aqueous phase containing Zn was discarded, the methylene chloride phase was re-extracted five times with 30 ml of water. After removal of the solvent (mostly water) about 6–8 g slightly orange to light brown material was obtained (average yield ca. 35%). Column chromatography on silica gel with a methylene chloride/ethanol gradient provided an almost colorless product.

Additional purification was done on a 5 ml solid phase extraction column (Chromabond C-18 100 mg column obtained from Macherey-Nagel, Düren, Germany) using a water/methanol gradient as the eluant. Colored solutions were subjected to the same procedure until the solution containing the *N*-oxides remained colorless.

The products were extracted three times with CH_2Cl_2, the solvent was removed and the identity and purity was checked, average yield: 25% (purified product).

The purity of the obtained products was assessed by TLC, HPLC, and UV–vis spectroscopy. Final identification of the purified products was performed by ^1H NMR, ^{13}C NMR, and IR spectroscopy. Purity was confirmed by microanalysis (see Table 3).

5.2.4. 5-Hydroxymethyl-5-methyl-pyrroline *N*-oxide

7 g of PMMPO (32.8 mmol) were dissolved in 10 ml water at 0 °C and 250 μl concentrated hydrochloric was added. The cleaving of the protective THP group was monitored every 10 min by HPLC. After completion, the solution was neutralized with stoichiometric amounts of solid sodium hydrogen carbonate and the organic impurities were extracted with 75% petroleum ether/25% CH_2Cl_2 (five times 15 ml, both phases checked by HPLC). The aqueous phase was evaporated carefully in a rotary evaporator at 35–40 °C and the product was dissolved in methylene chloride in order to separate the precipitated sodium chloride. Solid phase extraction on mini columns (5 g of C-18 material) yielded a purified material.

5.3. Instruments

NMR spectra were recorded on a Bruker Avance at 400 MHz for ^1H, and 100 MHz for ^{13}C at 22 °C. $CDCl_3$ was used as the solvent throughout, TMS (tetramethylsilane) as the internal standard. Concentrations were set to 10 mg sample/0.6 ml solvent, temperature to 293 K. ^{13}C peaks were assigned by means of APT (attached proton test), HMQC (^1H-detected heteronuclear multiple-quantum coherence) and HMBC (heteronuclear multiple bond connectivity) spectra. All chemical shift data are given in ppm units. Mass spectra were obtained on a ESI Q-TOF MS on a Waters Micromass Q-TOF Ultima Global in 70% aqueous methanol containing 0.1% formic acid at a flow rate of 5 μl/min. IR spectra were recorded as film on an ATI Mattson Genesis Series FT-IR spectrometer (see also Table 4).UV–vis spectra were recorded on Hitachi 150-20 and U-3300 spectrophotometers in double-beam mode against a blank of the respective solvent (Table 5). Determination of the concentrations was done measuring the absorption maxima in the range between 200 and 300 nm. For measurements of the partition coefficients, 500 μl of *n*-octanol was added to 500 μl of a solution of the respective spin trap (100 mM or 5–10 mg, respectively) in 100 mM phosphate buffer, pH 7.4. The mixture was vortexed for 2 min at room temperature. If necessary, the procedure was repeated several times, until an equilibrium between the two phases was achieved. After careful separation of the phases, the absorbance was read at the maximum around 235 nm after dilution with methanol. For EPR experiments, Bruker spectrometers (ESP300E and EMX) were used, operating at 9.7 GHz with 100 kHz modulation frequency, equipped with a rectangular TE_{102} or a TM_{110} microwave cavity. All calculations for spectral simulation were done using the SimFonia Program by Bruker (Table 6).

Acknowledgments

The authors wish to thank P. Jodl for skilful technical assistance in synthesis, purification, and characterization of the spin traps. The financial support of the Christian Doppler laboratory for advanced cellulose chemistry and analytics is gratefully acknowledged.

Supplementary data

Supplementary data associated with this article can be found, in the online version, at doi:10.1016/j.bmc.2010.11.052. These data include MOL files and InChiKeys of the most important compounds described in this article.

References and notes

1. Fréjaville, C.; Karoui, H.; Tuccio, B.; Le Moigne, F.; Culcasi, M.; Pietri, S.; Lauricella, R.; Tordo, P. *J. Med. Chem.* **1995**, *38*, 258.
2. Stolze, K.; Udilova, N.; Nohl, H. *Free Radical Biol. Med.* **2000**, *29*, 1005.
3. Stolze, K.; Udilova, N.; Nohl, H. *Biol. Chem.* **2002**, *383*, 813.
4. Stolze, K.; Udilova, N.; Rosenau, T.; Hofinger, A.; Nohl, H. *Biol. Chem.* **2003**, *384*, 493.
5. Stolze, K.; Rohr-Udilova, N.; Rosenau, T.; Stadtmüller, R.; Nohl, H. *Biochem. Pharmacol.* **2005**, *69*, 1351.
6. Stolze, K.; Rohr-Udilova, N.; Rosenau, T.; Hofinger, A.; Kolarich, D.; Nohl, H. *Bioorg. Med. Chem.* **2006**, *14*, 3368.
7. Stolze, K.; Rohr-Udilova, N.; Rosenau, T.; Hofinger, A.; Nohl, H. *Bioorg. Med. Chem.* **2007**, *15*, 2827.
8. Hardy, M.; Chalier, F.; Ouari, O.; Finet, J.-P.; Rockenbauer, A.; Tordo, P. *Chem. Commun.* **2007**, 1083.
9. Chalier, F.; Hardy, M.; Ouari, O.; Rockenbauer, A.; Tordo, P. *J. Org. Chem.* **2007**, *72*, 7886.
10. Hardy, M.; Rockenbauer, A.; Vasquez-Vivar, J.; Felix, C.; Lopez, M.; Srinivasan, S.; Avadhani, N.; Tordo, Paul.; Kalyanaraman, B. *Chem. Res. Toxicol.* **2007**, *20*, 1053.
11. Patel, A.; Rosenau, T.; unpublished results.
12. Baati, R.; Valleix, A.; Mioskowski, C.; Barma, D. K.; Falck, J. R. *Org. Lett.* **2000**, *2*, 485; cit. lit. Greene, T. W.; Wuts, P. G. M. *Protective Groups in Organic Synthesis*; Wiley: New York, 1999. Chapter 2, p. 57.
13. Mohammadpoor-Baltork, I.; Kharamesh, B. *J. Chem. Res. (S)* **1998**, 146; cit. lit.: Greene, T. W.; Wuts, P. G. M. *Protective Groups in Organic Synthesis*, 2nd ed.; Wiley: New York, 1991.
14. Karoui, H.; Rockenbauer, A.; Pietri, S.; Tordo, P. *Chem. Commun.* **2002**, 3030.
15. Bardelang, D.; Rockenbauer, A.; Karoui, H.; Finet, J.; Biskupska, I.; Banaszak, K.; Tordo, P. *Org. Biomol. Chem.* **2006**, *4*, 2874.
16. Han, Y.; Tuccio, B.; Lauricella, R.; Villamena, F. A. *J. Org. Chem.* **2008**, *73*, 7108.
17. Šnyrychová, I. *Free Radical Biol. Med.* **2010**, *48*, 264.
18. Zhang, H.; Joseph, J.; Vasquez-Vivar, J.; Karoui, H.; Nsanzumuhire, C.; Martásek, P.; Tordo, P.; Kalyanaraman, B. *FEBS Lett.* **2000**, *473*, 58.
19. Dikalov, S.; Jiang, J.; Mason, R. P. *Free Radical Res.* **2005**, *39*, 825.
20. Roubaud, V.; Lauricella, R.; Bouteiller, J. C.; Tuccio, B. *Arch. Biochem. Biophys.* **2002**, *397*, 51.
21. Stolze, K.; Rohr-Udilova, N.; Hofinger, A.; Rosenau, T. *Bioorg. Med. Chem.* **2008**, *16*, 8082.
22. Dikalov, S. I.; Mason, R. P. *Free Radical Biol. Med.* **2001**, *30*, 187.
23. Olive, G.; Mercier, A.; LeMoigne, F.; Rockenbauer, A.; Tordo, P. *Free Radical Biol. Med.* **2000**, *28*, 403.
24. Culcasi, M.; Rockenbauer, A.; Mercier, A.; Clément, J.-L.; Pietri, S. *Free Radical Biol. Med.* **2006**, *40*, 1524.